Supporting Information for

Predicted crystal energy landscapes of porous organic cages

Edward O. Pyzer-Knapp, Hugh P. G. Thompson, Florian Schiffmann, Kim E. Jelfs, Samantha Y. Chong, Marc A. Little, Andrew I. Cooper and Graeme M. Day

Details of Z'=2 crystal structure searches for **CC1**.

To test whether the observed β solvate framework of **CC1** would have been predictable, additional Monte Carlo simulated annealing searches were performed with two independent molecules in the asymmetric unit: one molecule in the most stable *T*-symmetry conformer and one molecule in the second lowest energy C_3-symmetry conformer. These searches were performed in space group $P3_2$, a subgroup containing all of the intermolecular symmetry operators of the observed space group (whose full space group symmetry, *R*3, includes intramolecular symmetry). All resulting structures were lattice energy minimised using the same force field + atomic multipoles energy model that was used for the Z`=1 predictions. To compare relative total lattice energies, the relative energy of the C_3 conformer was added to the calculated intermolecular energies from the DMACRYS calculations.

The lowest energy crystal structure resulting from this search reproduces the CC1 framework of the observed β solvate structure very well ($RMSD_{15}$ = 0.398 Å), see Figure S6.

Figure S1: Low energy conformations of cages CC3. Energies are from structures optimised at B3LYP/6-31G level of theory. A) lowest energy conformation, B) second lowest energy conformation.**

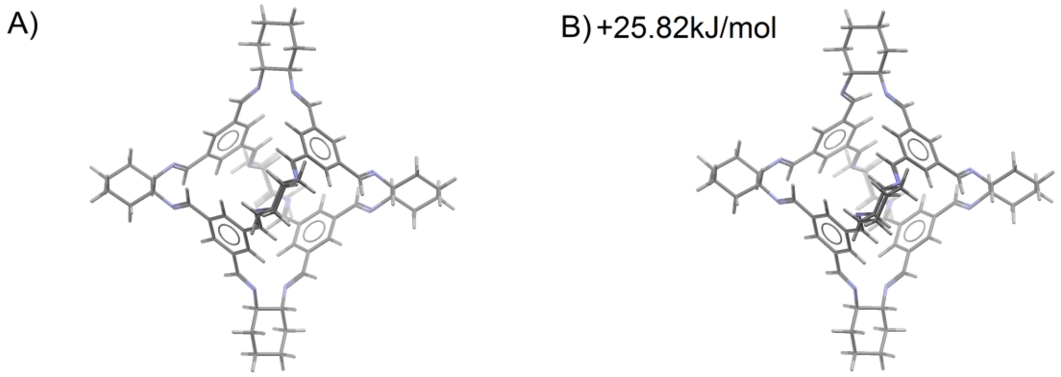

Figure S2: Low energy conformations of cages CC4. Energies are from structures optimised at B3LYP/6-31G level of theory. A) lowest energy conformation, B) second lowest energy conformation.**

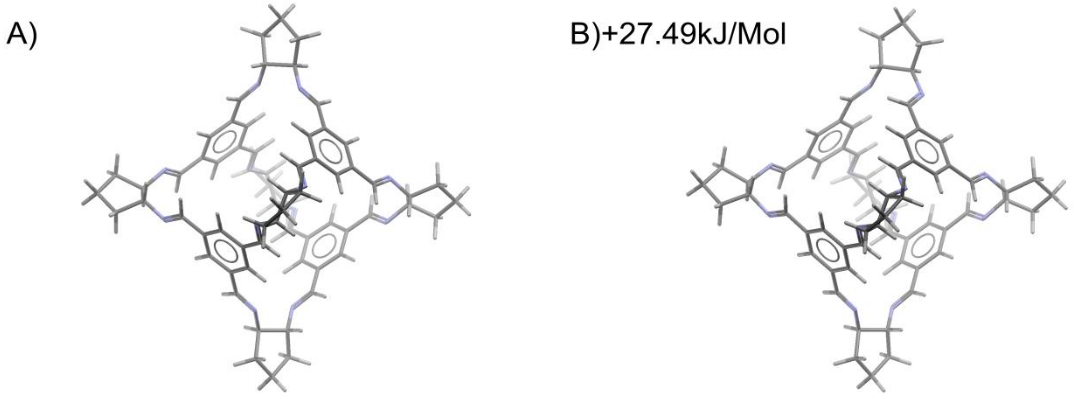

Figure S3: Low energy conformations of cages CC5. Energies are from structures optimised at B3LYP/6-31G level of theory. A) lowest energy conformation, B) second lowest energy conformation.**

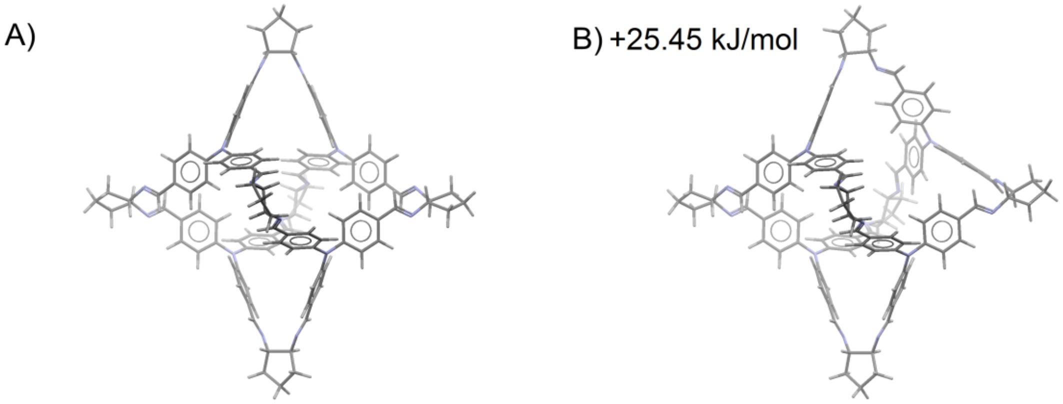

Figure S4: Crystal energy landscape for CC3 resulting from rigid molecule force field + multipoles lattice energy minimisation of hypothetical crystal structures. perimentally. Red points correspond to racemic crystal structures. Blue points are enantiomerically pure crystal structures. The observed structures correspond to the lowest energy CC3-*R* and CC3-*RS* predicted structures.

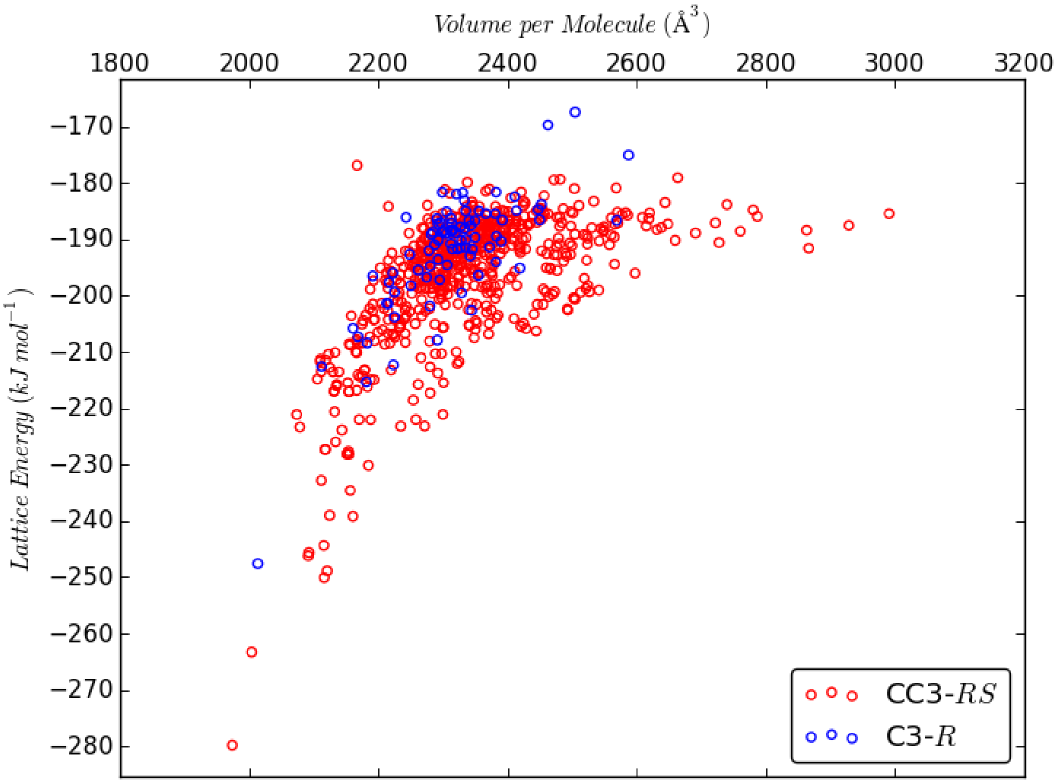

Figure S5: Crystal energy landscape CC5 resulting from rigid molecule force field + multipoles lattice energy minimisation of hypothetical crystal structures. Red points correspond to racemic crystal structures. Blue points are enantiomerically pure crystal structures. The observed structure corresponds to the lowest energy CC5-*R* predicted structure.

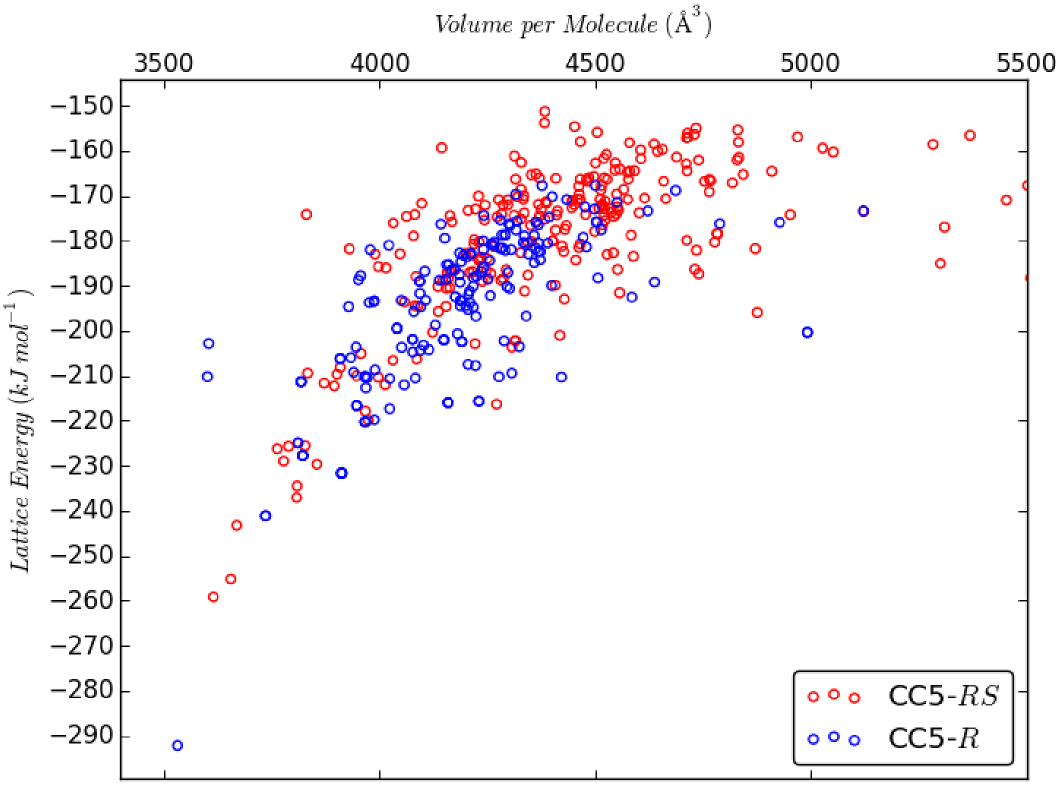

Figure S6: Overlay of experimental (red) and predicted (blue) CC1-β framework. The predicted framework is the lowest energy structure from a search with an asymmetric unit containing one of each of the two lowest energy predicted conformers. The overlays show the lowest attainable RMS when overlaying a cluster of 15 molecules.

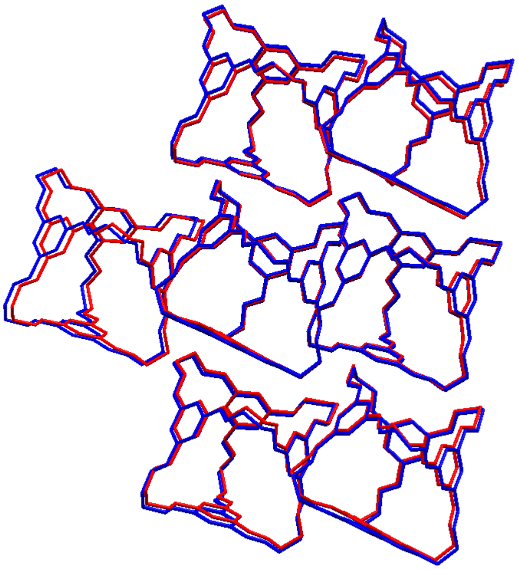

Figure S7: Overlay of experimental (red) and predicted (blue)for (A) CC3-*R* and (B) CC3-*RS* structures. The overlays show the lowest attainable RMS when overlaying a cluster of 15 molecules

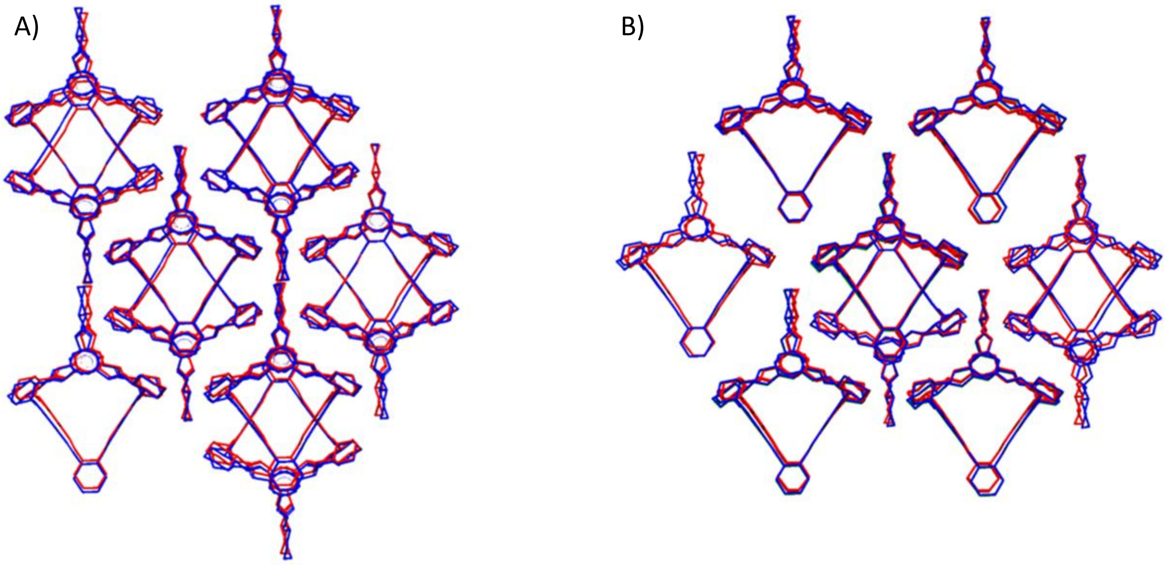

Figure S8: Overlay of experimental (red) and predicted (blue) CC5 structure. The overlays show the lowest attainable RMS when overlaying a cluster of 15 molecules

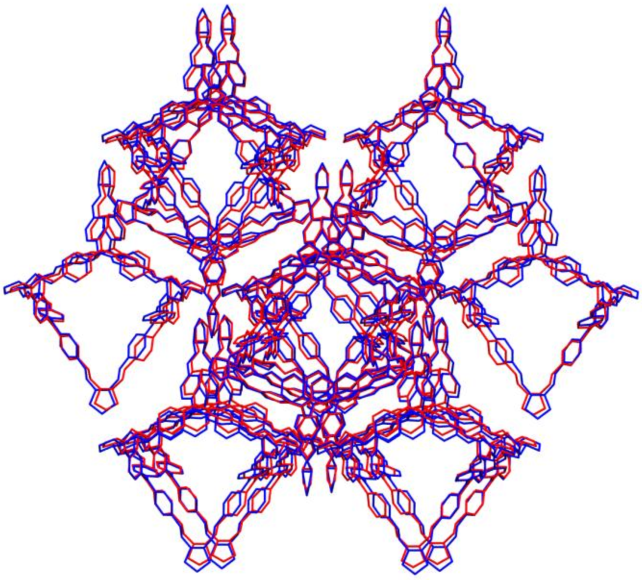

Figure S9: Comparisons of relative energies of CC1, CC3, CC4 and CC5 polymorphs as calculated by a rigid body force field +multipoles approach (DMACRYS) and a solid state DFT-D approach (CP2K). All energies are relative to the global minimum.

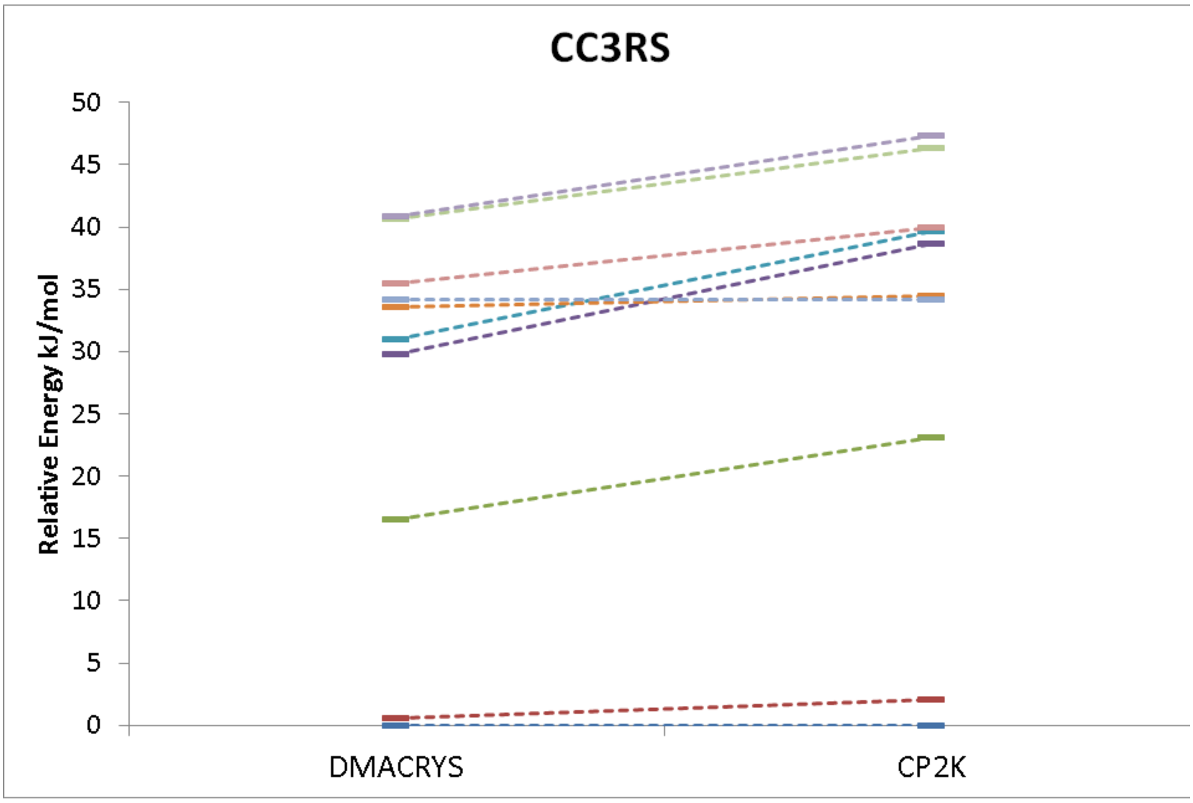

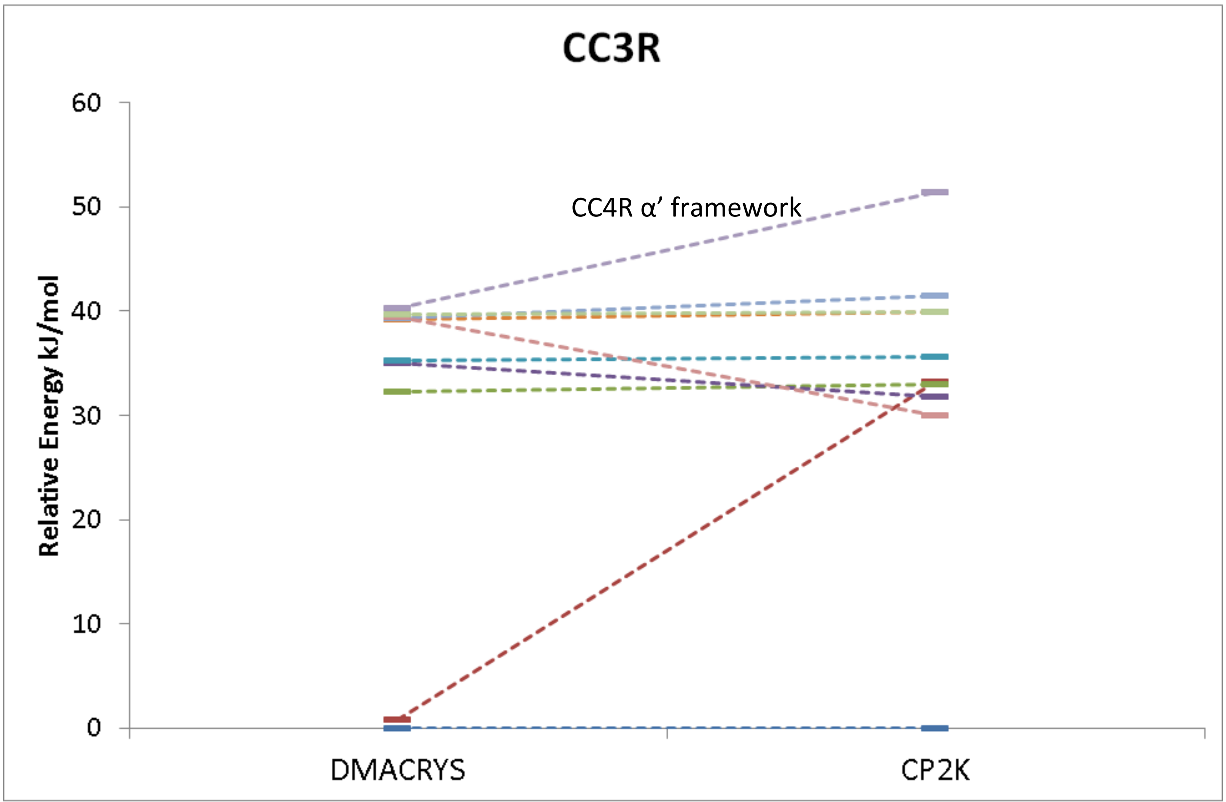
CC3R
Relative Energy kJ/mol
60
50
40
30
20
10
0
CC4R α' framework
DMACRYS
CP2K

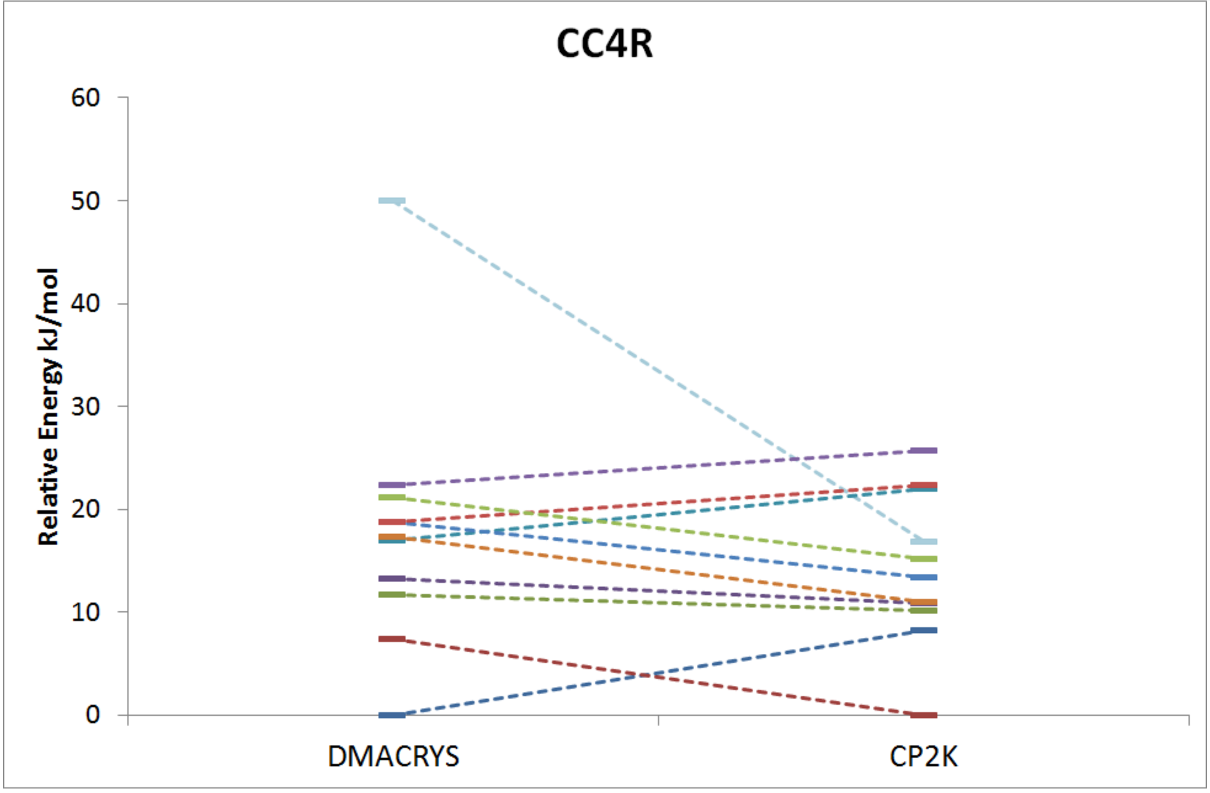
CC4R
Relative Energy kJ/mol
60
50
40
30
20
10
0
DMACRYS
CP2K

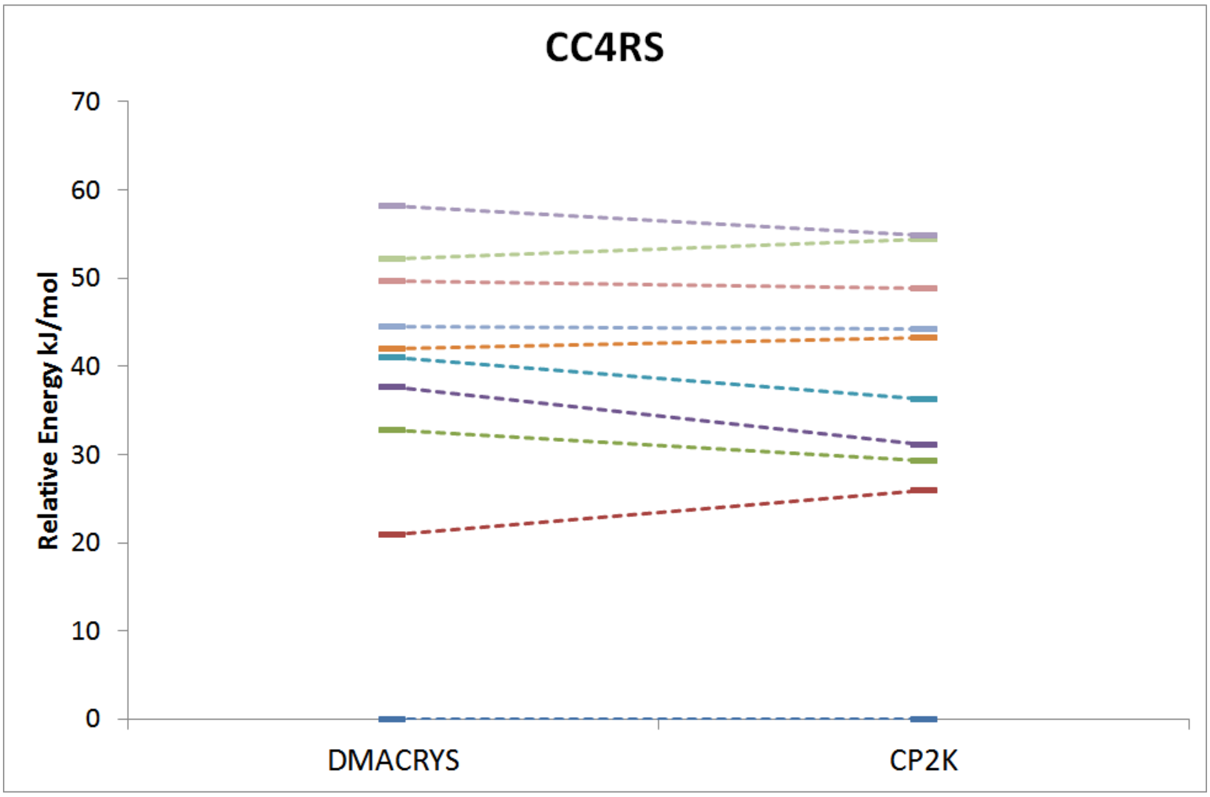
CC4RS
Relative Energy kJ/mol
70
60
50
40
30
20
10
0
DMACRYS
CP2K

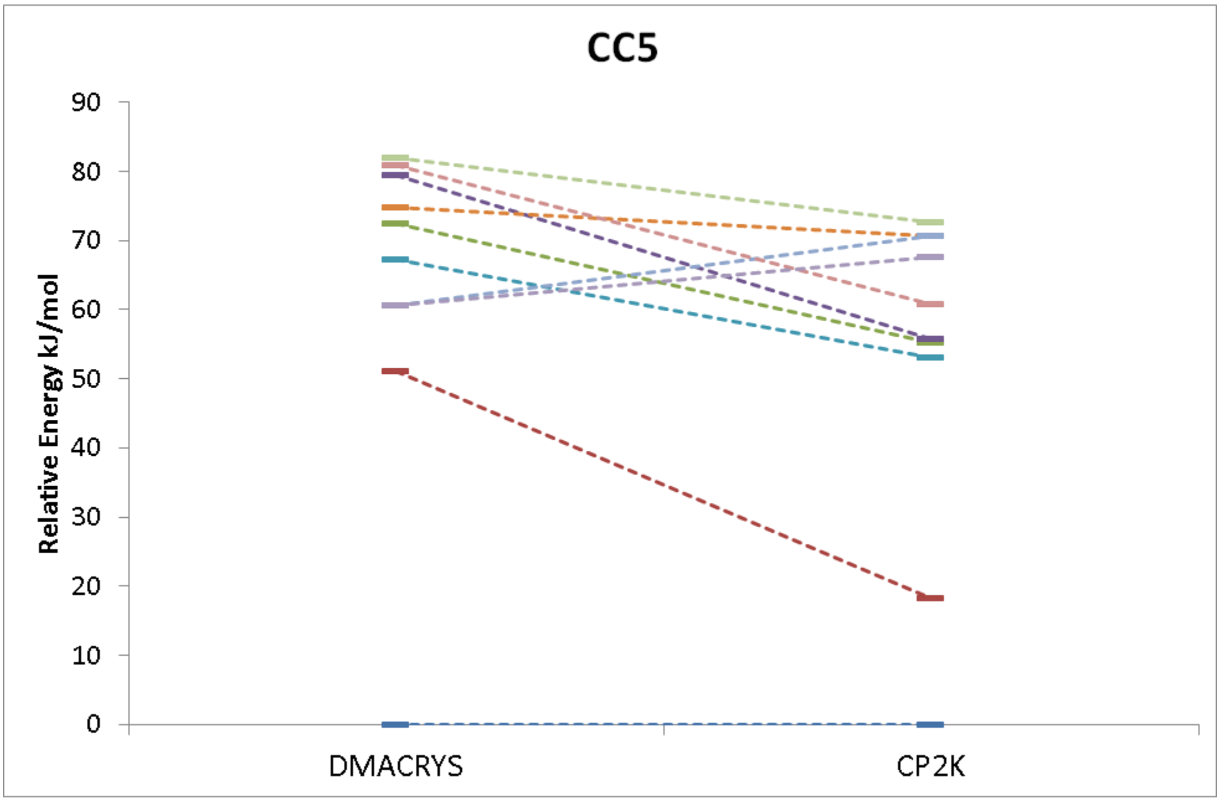
CC5
Relative Energy kJ/mol
90
80
70
60
50
40
30
20
10
0
DMACRYS
CP2K

Table S1: RMS Deviations in atomic positions of the molecule optimised in the gas phase (Gaussian), and the molecule optimised in the 10 lowest energy condensed phase structures (CP2K)

CC1	RMS (Å)
1	0.061
2	0.039
3	0.051
4	0.059
5	0.045
6	0.037
7	0.075
8	0.047
9	0.052
10	0.031
Mean	0.050

CC3-RS	RMS (Å)
1	0.023
2	0.028
3	0.024
4	0.034
5	0.026
6	0.024
7	0.024
8	0.02
9	0.033
10	0.041
Mean	0.028

CC4-RS	RMS (Å)
1	0.035
2	0.083
3	0.049
4	0.051
5	0.063
6	0.032
7	0.076
8	0.034
9	0.066
10	0.037
Mean	0.053

CC3-R	RMS (Å)
1	0.044
2	0.028
3	0.045
4	0.058
5	0.023
6	0.041
7	0.22
8	0.043
9	0.024
10	0.053
Mean	0.058

CC4-R	RMS (Å)
1	0.031
2	0.061
3	0.069
4	0.067
5	0.051
6	0.055
7	0.075
8	0.068
9	0.076
10	0.052
Mean	0.061

CC5	RMS (Å)
1	0.046
2	0.101
3	0.095
4	0.101
5	0.126
6	0.084
7	0.103
8	0.145
9	0.087
10	0.029
Mean	0.092

Figure S10: Comparisons of simulated powder patterns from the predicted (blue) and experimentally determined (red) crystal structures of A)CC1 α’ B) CC1 β’ C)CC3*R* D)CC3*RS* E)CC4*RS* and F)CC5*R*, simulated using a wavelength of λ = 1.54056 Å.

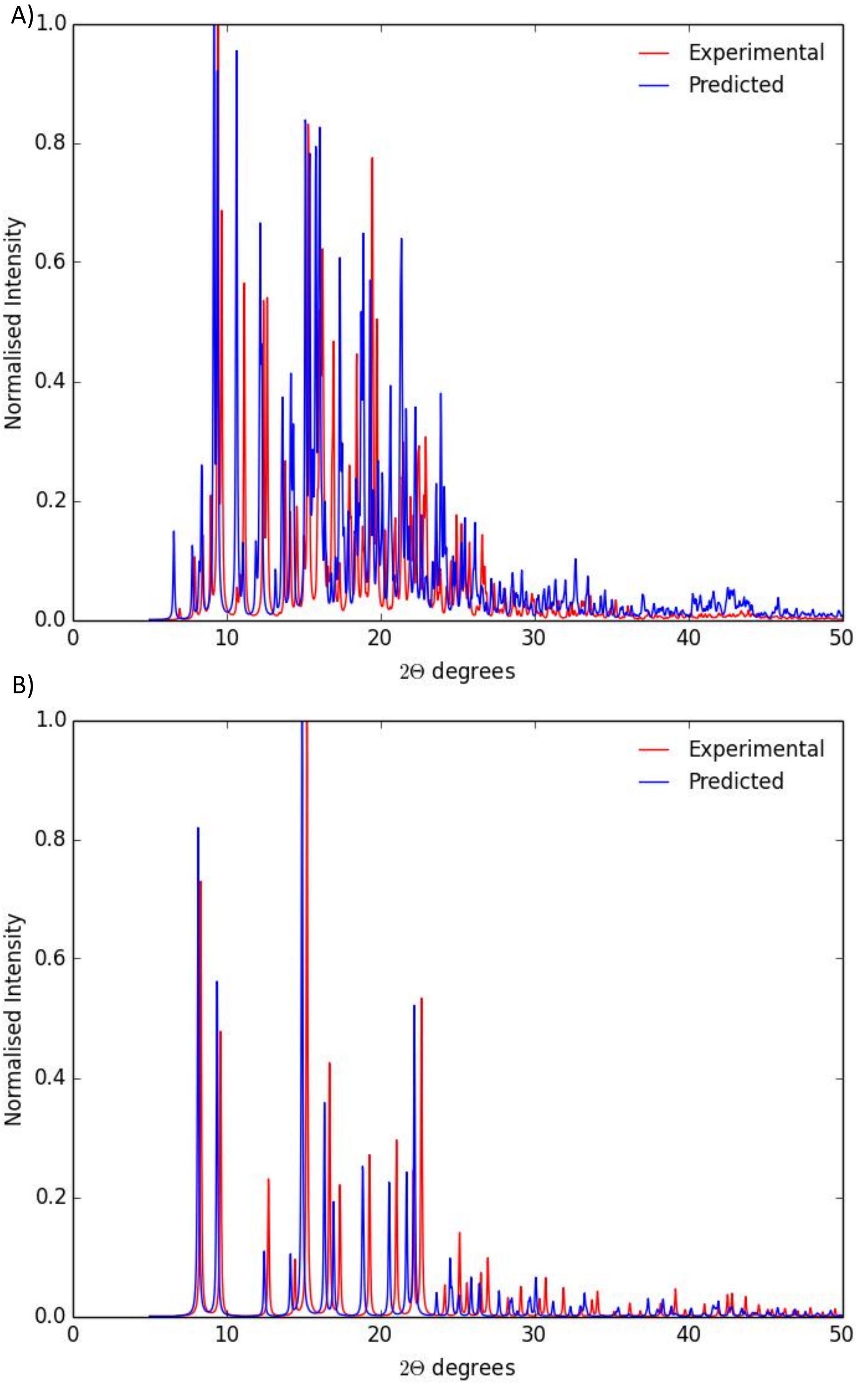

C)

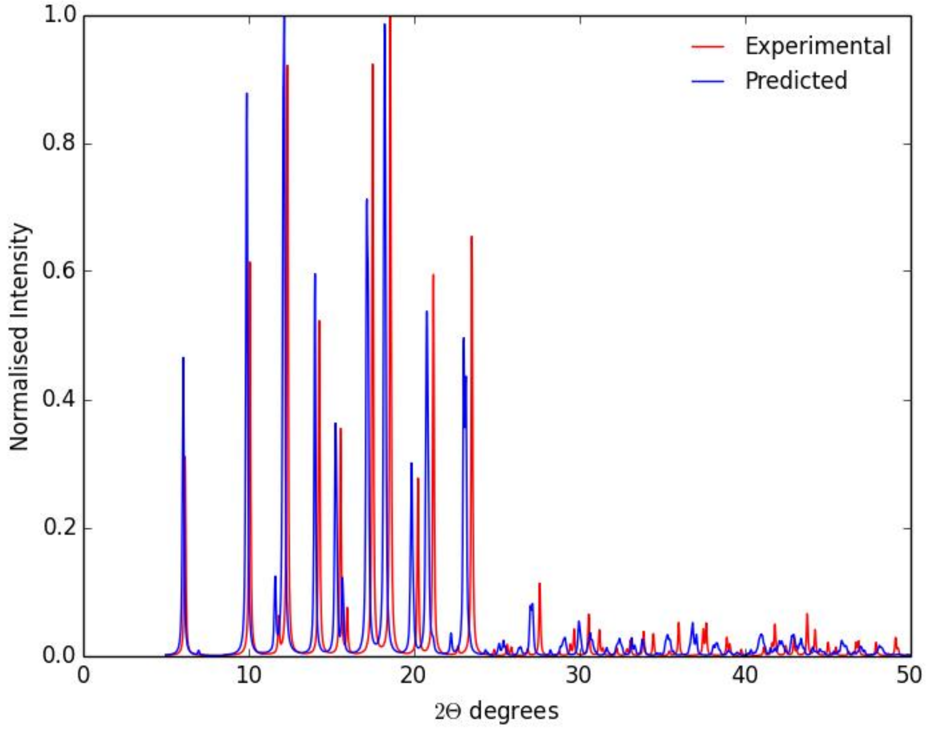

Experimental
Predicted
Normalised Intensity
0.0
0.2
0.4
0.6
0.8
1.0
0
10
20
30
40
50
2Θ degrees

D)

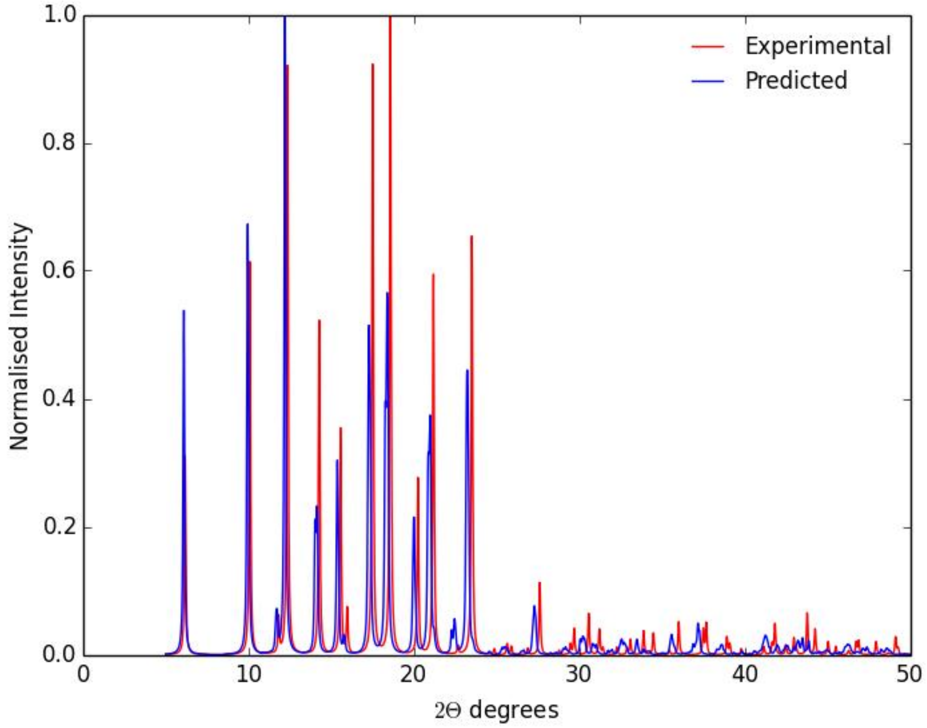

Experimental
Predicted
Normalised Intensity
0.0
0.2
0.4
0.6
0.8
1.0
0
10
20
30
40
50
2Θ degrees

E)

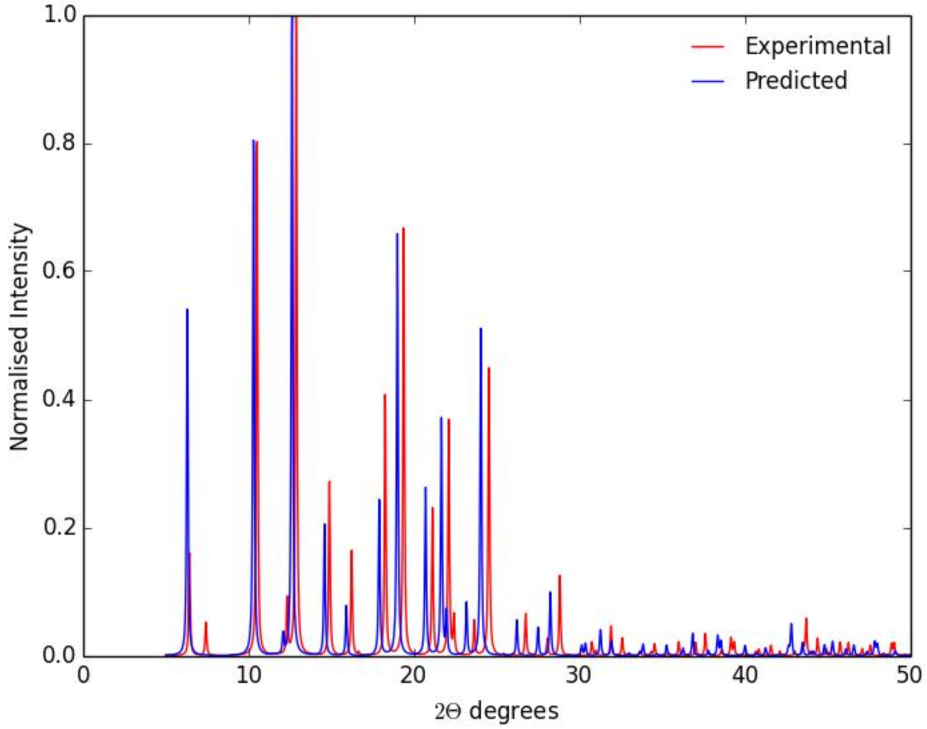

Experimental
Predicted
Normalised Intensity
1.0
0.8
0.6
0.4
0.2
0.0
0
10
20
30
40
50
2Θ degrees

F)

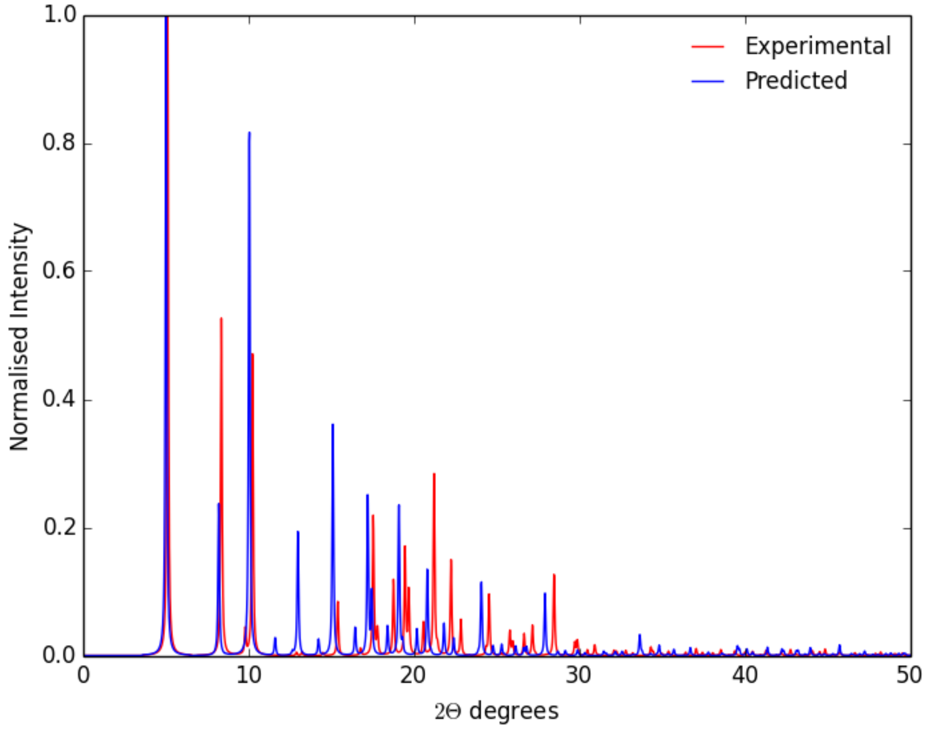

Experimental
Predicted
Normalised Intensity
1.0
0.8
0.6
0.4
0.2
0.0
0
10
20
30
40
50
2Θ degrees

Single Crystal X-Ray Diffraction. Data was measured on a Rigaku MicroMax-007 HF rotating anode diffractometer (Mo-Kα radiation, λ = 0.71073 Å, Kappa 4-circle goniometer, Rigaku Saturn724+ detector). An empirical absorption correction using equivalent reflections was performed with the program SADABS.[1] The structure was solved by direct methods using SHELXS,[2] and refined by full-matrix least squares on F^2 by SHELXL-97,[2] interfaced through the programme OLEX2.[3] All non-H atoms were refined anisotropically; H atoms were fixed in geometrically estimated positions using the riding model.

Single crystal preparation of **CC4**-*R* β′: A solvated single crystal of **CC4**-*R*·3(C_8H_{10})·2(H_2O) (space group $P2_12_12_1$, CCDC # 991219) isolated from a CH_2Cl_2/*para*-xylene solvent mixture and flash frozen at 100 K was very gradually heated under a dry N_2 gas stream to 350 K. The change in the sample temperature versus time was monitored using the plot shown in **Figure S11**.

Figure S11. Plot showing change in sample temperature versus duration of single crystal study carried out on flash frozen single crystal of CC4-*R*·3(C_8H_{10})·2(H_2O) (CCDC # 991219).

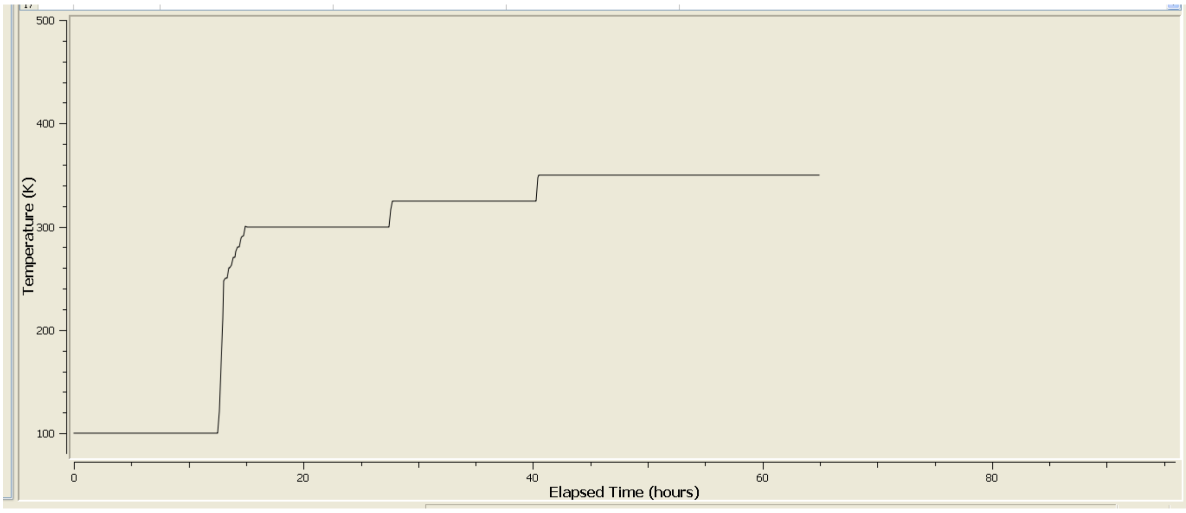

Crystal data for **CC4**-*R* β′. Formula $C_{66}H_{72}N_{12}$; M = 1033.36 g·mol^{-1}; cubic space group $F4_132$, colourless crystal; a = 24.242(9) Å; V = 14246(9) Å^3; ρ = 0.964 g·cm^{-3}; μ = 0.058 mm^{-3}; F (000) = 4416; crystal size = 0.41 x 0.17 x 0.04 mm^3; T = 350(2) K; 26 833 reflections measured (1.45 < Θ < 18.81°), 480 unique (R_{int} = 0.1241), 408 observed ($I > 2\sigma(I)$); R_1 = 0.1146 for observed and R_1 = 0.1270 for all reflections; wR_2 = 0.2692 for all reflections; max/min residual electron density = 0.956 and -0.191 e·Å^{-3}; data/restraints/parameters = 480/0/60; GOF = 1.338. CCDC # 991218

Refinement Notes for CC4-*R* β′. Desolvation of **CC4**-*R*·3(C_8H_{10})·2(H_2O) to afford **CC4**β is accompanied by a significant structural transformation. This results in a contraction of the unit cell volume per CC4-R molecule of ~ 14 % which greatly affects the single crystal data quality. The structure of **CC4**-*R* β′ was solved and refined in the chiral cubic space group $F4_132$. Diffuse scatter beyond a resolution limit of 1.1 Å was omitted during refinement. The asymmetric unit for **CC4**-*R* β′ is comprised of one twelfth of a **CC4**-*R* fragment. No restraints were used during refinement. For a displacement ellipsoid plot see **Figure S12**.

Figure S12. Displacement ellipsoid plot from the single crystal structure CC4-*R* β′, showing one complete CC4-*R* molecule.

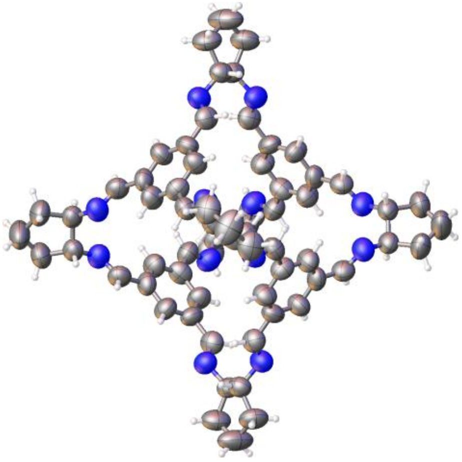

Bulk preparation of CC4-*R* β′ for PXRD analysis: To **CC4**-*R* (357 mg, 0.35 mmol) dissolved in CH_2Cl_2 (20 mL) *para*-xylene (30 mL) was carefully layered on top. The solvent mixture was allowed to slowly evaporate until only the last 5 mL remained. The remaining solvent was decanted and the isolated crystalline material was dried in a vacuum oven set at 90 °C for 18 hours. Isolated yield after evacuation 276 mg: 77 %.

Experimental powder X-ray diffraction (PXRD). PXRD data for **CC4**-*R* β′ were collected on a Bruker D8 Advance diffractometer producing Ge-monochromated Cu $K\alpha_1$ radiation equipped with a LynxEye position sensitive detector. The sample was contained in a 1 mm diameter special glass capillary and spun during data collection to improve powder averaging. Data were collected over the range $4 \leq 2\theta \leq 50°$ with a step size of 0.01° over 11 hrs using a variable counting time strategy.

References

1. G. M. Sheldrick, *(University of Göttingen, Germany)*, 2008.
2. G. M. Sheldrick, *Acta Cryst. Sect. A*, 2008, 64, 112-122.
3. O. V. Dolomanov, L. J. Bourhis, R. J. Gildea, J. A. K. Howard and H. Puschmann, *J. Appl. Cryst.*, 2009, 42, 339-341.